



Article

Big Rip Scenario in Brans-Dicke Theory

Sasmita Kumari Pradhan ^{1,2}, Sunil Kumar Tripathy ^{3,*}, Zashmir Naik ¹, Dipanjali Behera ³ and Mrutunjaya Bhuyan ^{4,*}

¹ School of Physics, Sambalpur University, Jyoti Vihar, Sambalpur 768019, India; sasmita.gita91@gmail.com (S.K.P.); zashmir@gmail.com (Z.N.)

² Department of Physics, Centurion University of Technology and Management, Bhubaneswar 751009, India

³ Department of Physics, Indira Gandhi Institute of Technology, Sarang, Dhenkanal 769146, India; dipadolly@rediffmail.com

⁴ Center for Theoretical and Computational Physics, Department of Physics, Faculty of Science, University of Malaya, Kuala Lumpur 50603, Malaysia

* Correspondence: tripathy_sunil@rediffmail.com (S.K.T.); bunuphy@um.edu.my (M.B.); Tel.: +91-8280295995 (S.K.T.); +60-1137057605 (M.B.)

Abstract: In this work, we present a Big Rip scenario within the framework of the generalized Brans-Dicke (GBD) theory. In the GBD theory, we consider an evolving BD parameter along with a self-interacting potential. An anisotropic background is considered to have a more general view of the cosmic expansion. The GBD theory with a cosmological constant is presented as an effective cosmic fluid within general relativity which favours a phantom field dominated phase. The model parameters are constrained so that the model provides reasonable estimates of the Hubble parameter and other recent observational aspects at the present epoch. The dynamical aspects of the BD parameter and the BD scalar field have been analysed. It is found that the present model witnesses a finite time doomsday at a time of $t_{BR} \simeq 16.14$ Gyr, and for this scenario, the model requires a large negative value of the Brans-Dicke parameter.

Keywords: cosmological constant; generalised Brans-Dicke theory; Big Rip



Citation: Pradhan S.K.; Tripathy, S.K.; Naik, Z.; Behera, D.; Bhuyan, M. Big Rip Scenario in Brans-Dicke Theory. *Foundations* **2022**, *2*, 128–139. <https://doi.org/10.3390/foundations2010007>

Academic Editor: Eugene Oks

Received: 16 December 2021

Accepted: 11 January 2022

Published: 17 January 2022

Publisher’s Note: MDPI stays neutral with regard to jurisdictional claims in published maps and institutional affiliations.



Copyright: © 2022 by the authors. Licensee MDPI, Basel, Switzerland. This article is an open access article distributed under the terms and conditions of the Creative Commons Attribution (CC BY) license (<https://creativecommons.org/licenses/by/4.0/>).

1. Introduction

Late-time cosmic acceleration is one of the most bizarre and unsolved problems in modern cosmology. In scalar field cosmological models, the late-time cosmic acceleration issue is predominantly attributed to an exotic dark energy (DE) form that corresponds to a cosmic fluid having low energy density, as well as negative pressure. This is usually understood through a quantity dubbed as the equation of state (EoS) parameter $\omega_D = \frac{p}{\rho}$, where p represents the DE pressure and ρ symbolises the dark energy density. The dark energy with a negative pressure corresponds to a negative EoS parameter. Despite several attempts made by astronomers and cosmologists, the experimental determination of ω_D remains challenging. Its precise estimation at the present epoch along with the knowledge of its development over a long period may unravel the mystery of the dark energy whose nature and origin remains speculative so far. In the Λ CDM model, the cosmological constant Λ with $\omega_D = 1$ plays the role of dark energy. However, in canonical scalar field models, quintessence fields or phantom fields shoulder the burden for the late-time cosmic speed-up, while the EoS parameter for the quintessence field lies in the range $-\frac{2}{3} \leq \omega_D \leq -\frac{1}{3}$ [1–3], which for the phantom fields, becomes $\omega_D < -1$ [4]. However, the EoS parameter as constrained from recent observational data favours a phantom phase in the Universe with $\omega_D < -1$ [5], while constraints from the CMB data in the nine-year WMAP survey suggest that $\omega_D = -1.073^{+0.090}_{-0.089}$ [6], a combination of the CMB data with Supernova data, predicts $\omega_D = -1.084 \pm 0.063$ [7]. Other constraints on the EoS parameter include $\omega_D = -1.035^{+0.055}_{-0.059}$ from Supernova cosmology project [8], $\omega_D = -1.03 \pm 0.03$ from recent Planck 2018 results [9] and from Pantheon data $\omega_D = -1.006 \pm 0.04$ [10].



Tunable room temperature ferromagnetism in fullerene thin film induced by 1 MeV proton microbeam irradiation

Ram Kumar^a, Krishna Mohan^a, Amala Augusthy^a, Sandeep Bari^b, Anukul P. Parhi^c, Aditya H. Kelkar^b, Sujay Chakravarty^d, Neeraj Shukla^{a,*}

^a National Institute of Technology Patna, Ashok Rajpath, Patna, Bihar 800005, India

^b Indian Institute of Technology, Kanpur, UP 208016, India

^c Indira Gandhi Institute of Technology, Sarang, Dhenkanal, Odisha 759146, India

^d UGC DAE CSR Kalpakkam Node, Kokilamedu, Tamil Nadu 603104, India

ARTICLE INFO

Keywords:

Ion irradiation
Microbeam
Ferromagnetism
Defects

ABSTRACT

We report tunable ferromagnetic properties of thin films of fullerene upon 1 MeV proton microbeam ion irradiation, by varying the ion fluence. Focused microbeam scanning of 1 MeV proton ions have been performed on the fullerene thin films. Consequently, a stable and significant ferromagnetic ordering at room temperature has been observed in the fullerene thin films. The proton microbeam irradiation induces a maximum magnetic ordering in fullerene with optimum dosage and subsequently higher fluence irradiations yield, diminishing effect upon the observed ferromagnetic ordering due to the higher degree of damages. The X-ray diffraction and Raman analysis confirm the damage due to proton microbeam irradiation. The reduction in the saturation magnetic moment induced, is very sharp as a result of exposure to the larger ion fluence. The approximate distance between defects has been simulated computationally, and its relation with observed ferromagnetism has been established. The irradiation has been performed at moderate ion flux (low microbeam current) to avoid the possible annealing effects of the ion irradiation.

1. Introduction

Ion irradiation over materials instigates significant and variable impact upon the properties of the materials viz; conductivity, phase transformation, surface energy, magnetization etc., depending upon the charge state, energy, ion flux, ion fluence & the angle of the impinging ion and the type of target sample [1,2]. The findings of weak ferromagnetism in transition metal free carbon related materials, have been of immense interest in the recent past [3–7]. One of the initial reports of weak ferromagnetism in a fullerene-based derivative of the charge-transfer salt, Tetrakis Dimethyl Amino Ethylene with Curie temperature around 16 K, was reported by Allemand et al. [8]. The ferromagnetism was observed at very low temperature and was explained on the basis of the correlated presence of unpaired π electrons in the sample. The carbon rich extraterrestrial meteorite, (found in Diablo Canyon), has also been reported to have weak ferromagnetism, where part of its weak ferromagnetic ordering is attributed to the proximity effects, related to the magnetic impurities in the sample [9]. The onset of room temperature ferromagnetism due to the optimized ion

irradiation in the metal free carbon related materials, has invited extensive interest of the scientific community in the last two decades [10–15]. Esquinazi et al. provided the first solid evidence of tunable ferromagnetic ordering in Highly Oriented Pyrolytic Graphite (HOPG), using 2.25 MeV proton beam irradiation [10]. The magnetism in carbon related materials viz; HOPG and carbon nanotubes etc., has largely been pinned on the magnetic correlations of the type of defects (vacancy/interstitial), presence of dangling bonds/adatom due to chemisorption, physisorption or hydrogenation and unique edge states etc. [6,7,16–19].

It has been reported, that the lighter ions (e.g., H^+ & He^+) are effective in creating defects in controlled manner and thus they induce almost similar magnetic response in graphite samples [20,44]. The proton and carbon ions are more versatile choice amongst lighter ions, as they can help in the realignment of under-coordinated bonds and these ions also have the additional advantage in ensconcing chemisorption and hydrogenation. Thus, the chemical nature of irradiating ions plays a very significant role in defect-based ferromagnetism. Further, it has been reported that the irradiation of the HOPG samples with the

* Corresponding author.

E-mail address: neerajs@nitp.ac.in (N. Shukla).

<https://doi.org/10.1016/j.tsf.2022.139350>

Received 20 November 2021; Received in revised form 15 June 2022; Accepted 15 June 2022

Available online 17 June 2022

0040-6090/© 2022 Elsevier B.V. All rights reserved.

transition metal elements viz; Fe⁺ ions, has failed to yield the desired result of inducing ferromagnetic ordering, as compared to that by the lighter ions [21]. The reason of this failure could be attributed to the fact, that the iron is much heavier than the proton or carbon atoms and creates 2–3 orders of extra damages in the materials with similar energy range even with very mild ion fluence.

The Buckminster fullerene material (another carbon allotrope, apart from HOPG and diamond) has also proved to be a fascinating material of interest since its discovery, due to its conspicuous properties, biocompatible nature and applications in possible electronic devices, in drug delivery, in cosmetics and as a gas sensor etc. [22–26]. The carbon allotrope in the form of fullerene (C₆₀) has a mixture of sp²-sp³ hybridization, with various Raman active modes and with each carbon atom covalently bonded with each neighboring carbon atom (multiple hexagon and pentagons formation), forming a closed football like structure. Fullerene samples can be readily functionalized, which further tailors its properties for various possible applications. One of the earliest reports of stable room temperature ferro-/ferri-magnetism in photo-polymerized fullerene (C₆₀), was reported as a consequence of exposure to photons of appropriate energy in oxygen atmosphere [27]. Wood et al. figured out, that the fullerene displays ferromagnetic properties under special sample environments (optimum high temperature and pressure) [28]. Although fullerene cage structure may not remain viable to above mentioned environments, and this may lead to the graphitization and functionalization of the fullerene [28]. Makarova et al. further reported, that the induced ferromagnetism can be controlled by laser exposure and electron beam irradiation and that the oxygen plays a contrasting role to the onset of ferromagnetic ordering in photo-polymerized and pressure polymerized fullerene derivatives [29,30].

As the energetic stream of lighter ions, have proved to be useful in curating ferromagnetic ordering in carbon related materials, it is worthwhile to explore its effect on the fullerene thin films [10]. The ion beam irradiation upon fullerene, results in changing a variety of its properties. The observation of 7 MeV ¹²C²⁺ ion irradiation upon fullerene thin film reveals that the conductivity of the sample increases as a function of ion fluence [31]. This experiment also establishes the role played by the variable ion fluences, in tuning the conductivity of the fullerene samples. Bajwa et al. have also explored the effect on the conductivity of fullerene thin film using swift heavy ion irradiation of 110 MeV Ni ions and they have revealed, that the samples irradiated with lower ion fluences, exhibit lower conductivity as compared to that in the case of samples irradiated with higher ion fluences [32].

The observation of ferromagnetism in fullerene samples by ion irradiation, have been reported by various research groups [33,34]. Kumar et al. have performed a comparative magnetization study of swift heavy ion irradiation (92 MeV Si⁺) and low energy (250 keV Ar⁺) ion irradiation upon fullerene thin films [33]. In the above work, the co-authors have reported weak ferromagnetic ordering in both the cases and they have highlighted the decisive role of the electronic energy loss and the nuclear energy loss related damages, in the observed magnetic ordering in the fullerene samples [33]. Matthew et al. observed significant ferromagnetic ordering in fullerene films by 2 MeV proton irradiation at 5 K only [34]. Lee et al. irradiated pelletized fullerene samples with broad proton beam [energy 0.5–2 MeV] of optimized ion fluence and demonstrated a room temperature ferromagnetic ordering of 0.173 A-m²/kg. Further, they have revealed, a magnetic field induced abrupt first order phase transition from ferromagnetism to diamagnetism [35]. These previous studies of the onset of ferromagnetic response in fullerene by ion irradiation, have revealed that the observed ferromagnetism has either been very feeble at room temperature or the corresponding Curie temperature has been significantly lower as compared to the room temperature or the observed magnetization undergoes phase transition with respect to higher magnetic field. Even the defects produced by neutrons in HOPG flakes, have been found to induce very low ferromagnetic behavior and strong paramagnetic behavior at low

temperature (1.8 K) [36]. The onset of ion beam induced room temperature ferromagnetism in carbon allotropes is in itself intriguing, apart from various possible futuristic applications. In the present work, we have found that 1 MeV proton microbeam enhances, the ferromagnetic ordering in the fullerene thin films significantly, even at room temperature. The observed ferromagnetism vanishes, if the samples are further irradiated to larger ion-fluences. The details of the observed room temperature ordering will be discussed in the subsequent sections.

2. Experimental

The fullerene thin films have been grown on SiO₂/Si substrate, through vacuum thermal evaporation utilizing a state-of-the-art deposition system equipped with multiple effusion cells. The deposition chamber has base pressure of 1.2×10^{-5} Pa, which rises up to 4.0×10^{-5} Pa during the evaporation. The doubly sublimed, purified fullerene (C₆₀) procured from Lumtec, has been utilized for the thin film deposition. The material is evaporated from one of the effusion cells at 460–470 °C to maintain the targeted deposition rate of 1 Å/s, with the help of an *in-situ* crystal thickness monitor. During deposition, the substrate temperature has been maintained at room temperature i.e. 25 °C. The film thickness to be grown is targeted at 1 μm. The typical size of the substrates has been kept about ~ 3 mm × 6 mm, compatible with both the Vibration Sample Magnetometer (VSM) samples holders and the microbeam irradiation chamber. The samples were irradiated with 1 MeV proton microbeam utilizing patterned microbeam scanning in the desired areas. The micro-beam line (Oxford Microbeam) attached to the 90° beam line of the 1.7 MeV Tandemron particle Accelerator (High Voltage Engineering, Europa, BV), was utilized at IIT Kanpur. The system provides focused microbeam ($Z \leq 6$) with spot size ranging from 1 – 20 μm. The focusing of the microbeam is achieved by electromagnetic quadrupole triplet based charged particle optics, working in Converging-Diverging-Converging (CDC combination). There are two high quality slits (objective and collimating) to control the beam spot and current at the sample. The micro-beam line also has the capability of ion scanning in desired shapes and sizes with the help of National Instrument (NI) 6259 PCI (Peripheral Component Interface) card and ION-SCAN software. The modulated X- and Y- output signals from the NI 6259 PCI card, are then amplified by a scan amplifier to maneuver ions ($Z \leq 6$). The signal from the scan amplifier is fed into an electromagnetic scanner, which maneuvers the focused microbeam ions on the target, in the desired shape and sizes. The samples were scanned with microbeam in a predefined area of (3.8 mm × 1.6 mm), chosen as per limitations of the sample size and scan amplifier constraints. The thickness of the deposited samples, has been assessed utilizing a surface Profilometer (DekTak 3, Bruker), to be about 1 μm.

The samples have been mounted in the microbeam chamber for the microbeam scanning, with chamber pressure maintained at about 2×10^{-4} Pa. As the CDC combination of quadrupole electromagnetic lenses, focuses the proton microbeam very sharply (very high beam current density), the micro-beam target current has been maintained between 20 and 22 nA to avoid possible annealing effects. A variable exposure of 1 MeV proton microbeam has been performed in the fluence range from 5.88 pC/μm² to 88.2 pC/μm². The Vibration Sample Magnetometer (VSM; Model EV-X DMS VSM, ADE Magnetics) has been utilized for the magnetic measurements at room temperature, at Advanced Center for Material Sciences, IIT Kanpur. The maximum applied magnetic field during the VSM measurement is ± 1.7 Tesla. The samples have been mounted on a non-magnetic quartz sample holder for VSM measurements. The VSM measurement has been repeated several times on sequentially irradiated samples to assess the effect of microbeam irradiation. The samples have been handled cautiously, utilizing Teflon tweezers in order to avoid exposure to any foreign contaminants viz; iron, cobalt etc. The samples have always been transported using covered vacuum desiccators from the accelerator laboratory to the VSM Laboratory for avoiding photopolymerization and moisture related

damages to the samples, if any.

The room temperature Glancing Incidence (angle of incidence 0.8°) X-ray diffraction (GIXRD), has been performed on some of the fullerene samples before and after irradiation on the GIXRD system (D8 Discover, Bruker), having rotating anode with 4.5 kW, Cu K_α source at UGC DAE CSR Kalpakkam node of Indore. A scintillation detector was used for GIXRD measurements. The effect of ion irradiation upon thin fullerene film has also been analyzed by Raman analysis (Renishaw InVia Raman Microscope excited by Argon Ion laser of wavelength 514 nm).

3. Results and discussion

3.1. Magnetization studies of un-irradiated and microbeam irradiated fullerene samples

The effect of 1 MeV proton microbeam scanning of appropriate fluence upon the thin films of fullerene, has been presented in Fig. 1. It shows the magnetization response to the applied field of both un-irradiated and irradiated fullerene samples. The un-irradiated sample shows, a very strong diamagnetic nature with negative slope, as expected. The sample shows, very promising response to the ion beam scanning with a fluence of $29.4 \text{ pC}/\mu\text{m}^2$, resulting in an appreciable ferromagnetic kink. This ferromagnetic kink is a manifestation of microbeam irradiation, in otherwise a strong diamagnetic fullerene sample. It is noteworthy, that the whole region of the sample has not been irradiated and only about 34% of the sample area, is exposed to the 1 MeV proton microbeam. There is a bulk SiO_2/Si substrate, underneath the thin fullerene film samples, and the overall sample has a strong diamagnetic nature. Further, this diamagnetic portion is subtracted using the slope of diamagnetic curves to explore the effect of ion beam irradiation. Five sets of similar sized samples have been utilized for ion beam irradiation by varying the irradiation fluence from $5.88 \text{ pC}/\mu\text{m}^2$ to $88.2 \text{ pC}/\mu\text{m}^2$, in the quest of exploring the optimized fluence for inducing maximum magnetic ordering in the sample. The VSM measurements performed on these samples, have been presented in Fig. 2, after the removal of the diamagnetic background.

It can be clearly seen in this figure, that at the lower fluence of $5.88 \text{ pC}/\mu\text{m}^2$, the observed saturation magnetic moment is $1.16 \times 10^{-7} \text{ A}\cdot\text{m}^2$, which is significantly higher than that for the un-irradiated sample. The maximum magnetization has been achieved at the fluence of $29.4 \text{ pC}/\mu\text{m}^2$. The observed coercivity in this sample is about 20 mT (millesla). The observed magnetization further decreases significantly, after increasing the ion fluence from $29.4 \text{ pC}/\mu\text{m}^2$ to $39.1 \text{ pC}/\mu\text{m}^2$. This larger fluence brought almost no change in the magnetization, as compared to

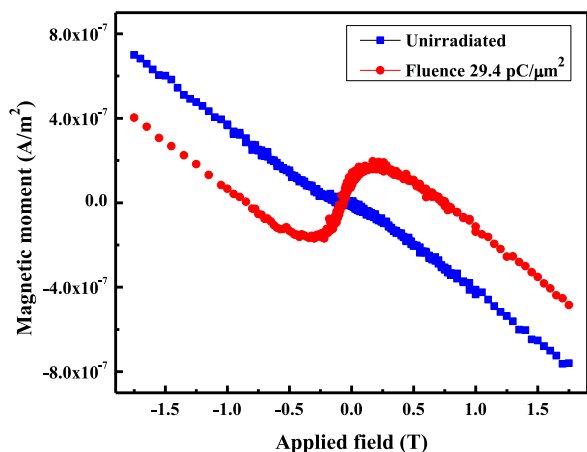


Fig. 1. Magnetic moment vs field measurement for unirradiated (C_{60}) and 1 MeV proton microbeam irradiated fullerene sample with fluence of about $29.4 \text{ pC}/\mu\text{m}^2$, showing a significant magnetization response of proton microbeam irradiation.

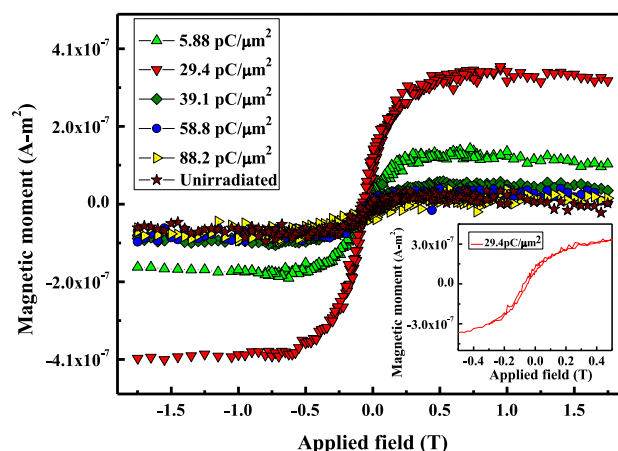


Fig. 2. Magnetic moment of un-irradiated (C_{60}) specimen and irradiated specimens with ion fluence irradiation range of $5.88\text{--}88.2 \text{ pC}/\mu\text{m}^2$, after subtracting the diamagnetic contribution (inset showing the hysteresis in the sample irradiated with ion fluence of $29.4 \text{ pC}/\mu\text{m}^2$).

the un-irradiated sample data. The saturation magnetization further decreases monotonically, for the fluences of $58.8 \text{ pC}/\mu\text{m}^2$ and $88.2 \text{ pC}/\mu\text{m}^2$. This shows that the observed maximum ferromagnetic ordering in the fullerene thin film, favors an optimum ion fluence window.

The saturation magnetic moment data vs the total charge irradiated in the microbeam scanning, has been shown in Fig. 3. The saturation magnetic moment has been derived from the data reported in Fig. 2. We can observe that the saturation magnetization is maximum for the total charge irradiation of $183.5 \mu\text{C}$, corresponding to the ion fluence of $29.4 \text{ pC}/\mu\text{m}^2$. Fig. 3 also enunciates, that there is a threshold window of total charge irradiation, during which, the observed saturation magnetization is maximum. Fig. 3 also unravels the information, that below and above the threshold ion fluence window, the observed magnetization is much lower and that at the higher total charge irradiation, diminishes gradually. However more data points would be required to reveal the peak of the optimum fluence.

3.2. Structural analysis of unirradiated and irradiated fullerene sample

The GIXRD data for the unirradiated and the irradiated samples (where the induced magnetization was maximum), are shown in Fig. 4 (a). This figure describes, that the unirradiated sample has all the characteristic peaks of fullerene, with the highest intensity peaks (0 0 2) and (1 1 2). The observed peaks matches well with JCPDS (card no. 00-047-0787) data for fullerene. The GIXRD data for the unirradiated

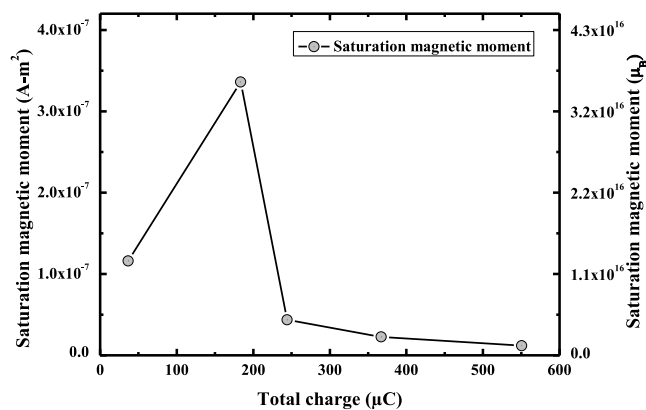


Fig. 3. Dependence of the saturation magnetic moment (in $\text{A}\cdot\text{m}^2$ and Bohr magneton (μ_B) unit) vs the total irradiated charge (μC), depicting a threshold fluence window for maximum magnetization.

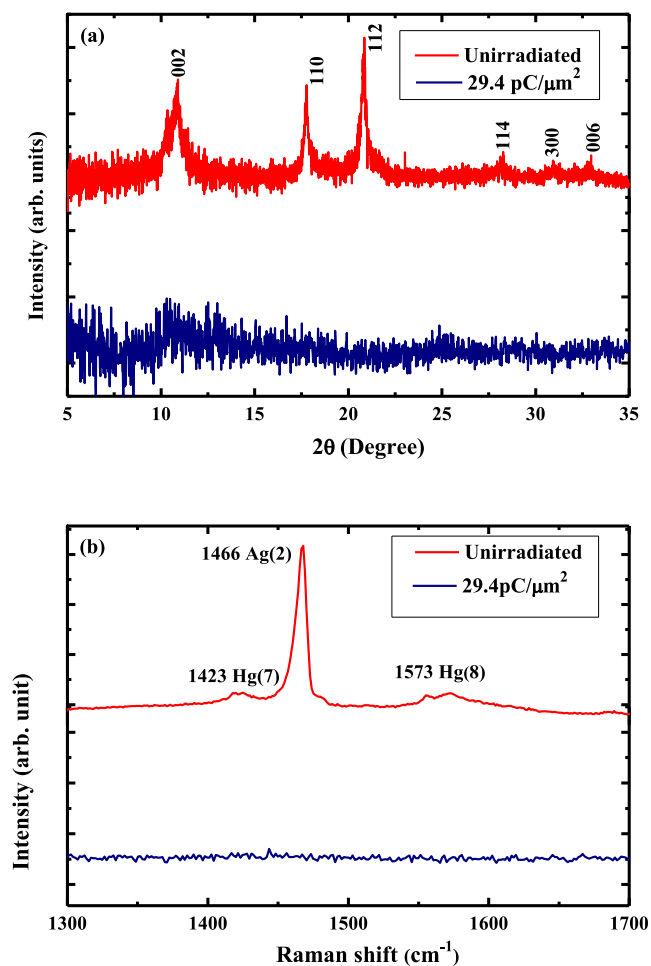


Fig. 4. (a) GIXRD data and (b) Raman data exhibiting significant damage in the irradiated sample with fluence $29.4 \text{ pC}/\mu\text{m}^2$ as compared to the unirradiated sample.

sample (fluence $29.4 \text{ pC}/\mu\text{m}^2$) shows remarkable decrease in the intensity of characteristic fullerene peaks, which is indicative of excessive ion beam induced damage. The data analysis of the observed peaks, indicate that the crystallite size for unirradiated sample is about 7 nm and that for irradiated sample ($29.4 \text{ pC}/\mu\text{m}^2$) is about 31 nm. The irradiated samples clearly show the signatures of significant damage to the fullerene structure even with mild fluences, with significant decrease in the intensity of the noteworthy peaks and only one peak (0 0 2) barely survives the ion fluence of $29.4 \text{ pC}/\mu\text{m}^2$. Thus there is a significant damage due to ion beam irradiation in the fullerene thin film, which is also reflected in the Raman data of the same samples as shown in Fig. 4 (b). Fig. 4(b) shows the characteristic Raman modes of the unirradiated thin film fullerene and the 1 MeV proton microbeam irradiated samples ($29.4 \text{ pC}/\mu\text{m}^2$). The unirradiated sample reveals the presence of Hg (7) mode at 1423 cm^{-1} , Ag (2) mode at 1466 cm^{-1} and Hg (8) mode at 1573 cm^{-1} . The Raman modes disappear completely post 1 MeV proton microbeam irradiation, indicating significant damage to the cage structure.

3.3. Simulation of the ion beam induced damages in fullerene sample and discussion

In collision between an energetic proton and atoms in a solid, energy from the projectile is dissipated to the atoms (to the nucleus or electrons depending the energy of the projectile). Once the recoiling atoms of the target material acquire enough energy to leave their position within the

atomic network, various defects at the atomic scale may appear. While many defects such as vacancy-interstitial pair may disappear within seconds of the ion beam impact, some may remain in the system and form a more complicated defect structure. The onset of ferromagnetic ordering, as a consequence of ion irradiation upon various samples under various circumstances (change of ion, energy etc.) has been attributed to the creation of vacancies, unpaired electrons of dangling bonds and chemisorbed atoms etc. [7,11]. Therefore, the understanding of the ion beam induced damage assessment, in the present case becomes very crucial in order to gain an insight into the observed ferromagnetic ordering. We have performed the Stopping Range of Ions in Matter (SRIM) simulation for 1 MeV proton in fullerene [37–39]. We have calculated the range of the 1 MeV proton in carbon C_{60} target using SRIM, which was found to be about $16.87 \mu\text{m}$ and our specimen film is $1 \mu\text{m}$ thick. Therefore, the protons transmitted through the film, settle into the bulk silicon substrate [37]. The total energy loss of the proton microbeam in C_{60} film, has been calculated to be about 52 keV as per SRIM data analysis [37]. Esquinazi et al. [10] and Lehtinen et al. [11] have shown, that the proton beam created vacancies plays a major role in ion induced magnetic ordering in HOPG samples and the claims are supported by density functional theory as well.

1 MeV proton ions create roughly 14 vacancies per ion in the fullerene thin films as per SRIM analysis. The distance between defects estimated from the vacancy density as a function of the total charge irradiated, has been shown in Fig. 5, which exhibits that the distance between defects (considering uniform distribution) decreases as the total irradiated charge increases. This indicates that the sample sequentially leads towards amorphization. The distance between defects, is around 3.4 nm, corresponding to the ion fluence of $29.4 \text{ pC}/\mu\text{m}^2$ (Fluence of maximum/significant ferromagnetic ordering). Correlating the data from Figs. 3 and 5, it can be observed, that the measured ferromagnetism in fullerene samples vary as per distance between defects. It can be noted that the induced magnetic response is similar in the lower and the higher side of the fluence. In the former case, the distance between defects, is very large and these random sparse defects do not contribute significantly to the onset of magnetic ordering. On the other hand, in the latter case i.e. in highest fluence irradiated samples, defects come so close that they completely amorphize the sample, which again negates any possible correlation between defects leading to the poor magnetization. The higher ion-fluence irradiation would create more defects in the fullerene structure e.g., collapse of cages, fragmentation, presence of dangling bonds and point defects. As ion-fluence is increased

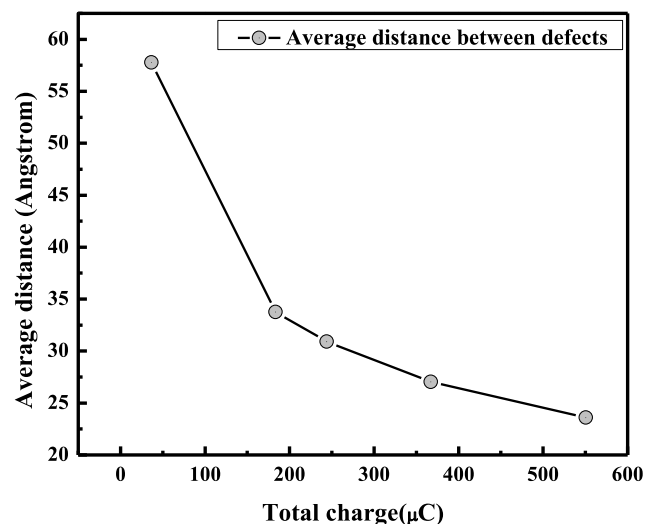


Fig. 5. Average distance between defects as a function of total charge irradiated, showing sharp decrease in the distance between defects as the total irradiated charge increases.

further, the structure of the fullerene maybe destroyed completely. If the level of damage increases beyond a certain limit as shown in Fig. 5, magnetic ordering of the sample decreases due to the complete amorphization/un-correlation of defects in the sample. The maximum saturation of magnetic moment corresponds to 183.55 μC of total charge irradiation with the fluence of 29.4 $\text{pC}/\mu\text{m}^2$. The maximum magnetic moment induced by 1 MeV proton microbeam is of order of $\sim 10^{-7} \text{ A}\cdot\text{m}^2$, at room temperature as shown in the Fig. 3.

The proton irradiation leads to the hydrogenation/chemisorptions in carbon allotropes as well as vacancy creation. The hydrogen chemisorptions and the carbon vacancy are equivalent in terms of one orbital model and induce similar magnetic moment. The density of state calculations for chemisorbed impurity (resulting in localized π electron near zero-point energy) in hexagonal graphene reveals a strong localized density of state near zero point energy. The density of state for such quasi-localized state due hydrogen chemisorptions is stronger than that for vacancy defect in graphene layers [7]. The localization length of quasi-localized π electrons as a consequence of defects in graphene is around 3–10 nm [40]. Assuming this to be applicable to the hexagonal rings of fullerene, the π electron interaction can extend to nearest neighbor fullerenes, which may result in exchange interaction leading to the observation of net room temperature ferromagnetic ordering. Thus, the observed ferromagnetism in the sample can be related as a correlated exchange response between defects placed at moderate and optimum distances (3.4 nm) as observed from Fig. 5 for the optimum fluence/maximum magnetization.

Kumar et al. have reported the onset of magnetic ordering in fullerene samples, by 92 MeV Si^+ ions and the same by 250 keV Ar^+ ions irradiation with variable fluences [33]. The observed magnetic moment ($\sim 10^{-8} \text{ A}\cdot\text{m}^2$) was one order lower than that found in the present experiment ($\sim 10^{-7} \text{ A}\cdot\text{m}^2$). The reason of not getting appreciable ferromagnetic ordering by Kumar et al. at lower energy of 250 keV Ar^+ ions, could lie in the fact that at low ion energy, the lateral straggling effects are significant as compared to that by higher energy ions. The higher atomic number ions create more vacancy per incident ions as compared to lower atomic number (Z) ions. It has been calculated from SRIM simulations that, 1 MeV protons will create 14 vacancies/ion, while 92 MeV Si^+ ion creates 2632 vacancies/ion in fullerene samples [37–39]. This difference could be the reason for better controlled defect generating capability of proton ions and other lower atomic number (Z) ions, in fullerene, as compared to that by heavier ions in MeV range. S. Mathew et al. have also reported the magnetization in fullerene at low temperature (5 K) using 2 MeV proton beam [34] and their broad beam irradiation could not lead to room temperature magnetic ordering the thin fullerene film. Lee et al. have observed a remarkable field induced transition from ferromagnetic ordering to diamagnetic ordering in broad proton beam irradiated pelletized fullerene samples in the energy range 0.5 MeV–2 MeV with variable ion fluence [35]. The sample which showed a significant response to ion beam irradiation was with broad proton beam energy of 0.5 MeV and ion fluence of $1 \times 10^{13} \text{ H}^+/\text{cm}^2$. It was further demonstrated that the observed ferromagnetism in fullerene pellets retains its induced ferromagnetic order in low magnetic fields only, and as the magnetic field is increased, there is an abrupt first order phase change from ferromagnetism to diamagnetism. Lee et al. have attributed the observed magnetization of $0.173 \text{ A}\cdot\text{m}^2/\text{kg}$, to the spin $S = 1$ contribution from defects related to the carbon vacancies and the hydrogen chemisorptions [35]. Though the observed magnetic ordering is smaller, but the nature of magnetic field-based phase switching is very interesting phenomenon. The microbeam utilized in the present experimentation, has an advantage of focused beam and desired pattern irradiation, thereby it produces a tunable, induced ferromagnetic ordering in the desired region. The observed ferromagnetic contribution from the irradiated thin fullerene volume (for 29.4 $\text{pC}/\mu\text{m}^2$ ion fluence) in our experiments comes out to be about $32.2 \text{ A}\cdot\text{m}^2/\text{kg}$ under optimal irradiation, which is very higher than that reported by Lee et al., for fullerene pellets ($0.173 \text{ A}\cdot\text{m}^2/\text{kg}$). The main feature of the present result,

lies in the fact that the observed magnetic ordering is significant even at room temperature in fullerene thin film and shows no signs of field-based phase switching.

The effect of energy variation upon inducing magnetic ordering in samples, has not been explored in details, but possible inferences could be drawn from the work of others. A noteworthy example, is the comparison of work of Xia et al. [13] and Shukla et al. [15]. Xia et al. have reported an order of magnitude lesser magnetic ordering ($\sim 10^{-8} \text{ A}\cdot\text{m}^2$) using 70 keV carbon ion irradiation on HOPG as compared to 1 MeV carbon microbeam irradiation on HOPG reported by Shukla et al. ($\sim 10^{-7} \text{ A}\cdot\text{m}^2$). Here the reason for this difference could be pinned on the fact that the keV- ranged carbon ions create, a significant amount of damage near the surface as compared to 1 MeV $^{12}\text{C}^+$ carbon ions in HOPG, due to the significant nuclear energy loss near the surface for keV- ranged ions, and electronic energy loss for MeV- ranged ions. One of the first reports of ion beam induced magnetic ordering in HOPG by 2.25 MeV proton ion irradiation, yielded the magnetic moments of the order $\sim 10^{-9} \text{ A}\cdot\text{m}^2$ [10]. Very high energy ions have another disadvantage of self-annealing of defects along the ion track due to heating effects of the ion beam. This is very crucial aspect and cannot be ignored while performing experiments at higher ion fluxes. Thus, by these comparisons, it is clear in the case of HOPG that the intermediate energy values of ions, turns out to be more useful in creating ferromagnetic ordering. The average magnetic moment induced in the sample, has been estimated in terms of the equivalent Bohr magneton (μ_B) per incident ion. The maximum magnetic moment induced is $31.6 \mu_B/\text{ion}$. Similar experiments by 70 keV and 1 MeV carbon ion irradiation upon HOPG produced the magnetic moment of about $41 \mu_B/\text{ion}$ and $60 \mu_B/\text{ion}$, respectively [13,15].

The samples have been irradiated at normal incidence to increase the chances of channeling in the crystalline Si substrate, precisely to rule out relatively larger damage in Si and avoiding any possible effect of damage to the Si substrate in the observed ferromagnetic ordering. Usually to avoid channeling effects (to maximize the damage), the Si/SiC substrates are kept at off normal (by 7°) orientations [41,42,]. The Silicon atom ($Z = 14$) is heavier than carbon atom in Fullerene ($Z = 6$) and as per SRIM calculations, 1 MeV proton ions would create lesser damage in Si than in Fullerene (The displacement energy for Si being larger than that for Carbon in fullerene). The damage in the silicon substrate is also limited due to higher order of channeling in normal irradiations. Thus, taking these precautions, it is inferred that the effect is primarily due to thin fullerene films only.

One more crucial aspect to consider while tailoring the defect density, is the heating effects of the ions beam upon the sample, as mentioned earlier. Since the *in-situ* annealing of the defects along the ion beam path might have detrimental effect on the magnetic correlations of the defects, the microbeam irradiation was performed, maintaining lower ion beam current in the range 20–22 nA throughout the experiment. An estimation of the temperature rise, due to ion beam irradiation solving the heat conduction equations, considering the possible dissipation through radiation and conduction in the sample, can be easily made. The calculations reveal, that the parameters of the microbeam (1 MeV, 20 nA) in the present experiment, would create an equilibrium temperature of about 326 K near the end of the ion range, which is insignificant for the annealing of defects. This temperature is much smaller than the possible annealing temperature in Stoner-Waals type of defects in Fullerene [43]. Therefore, the self-annealing of defects and their transformation into other forms in the present work, does not arise, as the ion fluences were administered with lower beam currents resulting in mild temperature rise.

4. Conclusions

In conclusion, 1 MeV proton microbeam ion irradiation is capable of inducing a stable and significant room temperature ferromagnetism in fullerene with optimum dose of 29.4 $\text{pC}/\mu\text{m}^2$. The results also reveal that

the observed ferromagnetic ordering, is maximum within a threshold window of fluence and the total charges irradiated. The observed magnetic ordering is negligible below and beyond the threshold window of fluence and total charge. We have found the induced magnetic moments to be of the order of $31.6 \mu_B/\text{ion}$ for 1 MeV proton microbeam irradiation in Fullerene thin film. The advantage of utilizing the intermediate energy (1 MeV) of proton microbeam resulted in room temperature ferromagnetic ordering in the fullerene thin film. The optimum energy for creating best possible magnetization in fullerene, can be sought in future analysis, as this is also a suitable and important parameter in the quest for maximum magnetization in Fullerene. The advantage of microbeam resulted in the controlled irradiation of the sample area. The observed magnetization at optimized ion-fluence, grants us a unique recipe for creating ferromagnetic ordering in desired zones only. Thus, the present experiment could lead the way in creating a desired magnetic pattern on the thin films of fullerene, which can find applications in the preparation of light weight magnet, memory devices and many other future applications etc. at the room temperature.

CRedit authorship contribution statement

Ram Kumar: Conceptualization, Methodology, Investigation, Data curation, Validation, Formal analysis, Writing – original draft, Writing – review & editing. **Krishna Mohan:** Validation. **Amala Augusthy:** Validation. **Sandeep Bari:** Investigation. **Anukul P. Parhi:** Resources. **Aditya H. Kelkar:** Investigation, Writing – review & editing. **Sujay Chakravarty:** Investigation. **Neeraj Shukla:** Conceptualization, Resources, Investigation, Formal analysis, Writing – original draft, Writing – review & editing, Supervision, Project administration.

Declaration of Competing Interest

The authors declare that they have no known competing financial interests or personal relationships that could have appeared to influence the work reported in this paper.

Data availability

Data will be made available on request.

Acknowledgments

We gratefully acknowledge the financial support provided by Department of Science and technology New Delhi (Grant no DST/INSPIRE/04/2014/002647) and UGC-DAE CSR Kalpakkam node of Indore (Grant no CRS-KN/CRS-109/2018–19). We also acknowledge the technical support provided by Mr. M. Siva Kumar and Mukesh Kumar for VSM measurements at Advanced Center for Materials Sciences, IIT Kanpur. We also acknowledge the generous support from Tandatron accelerator facility at IIT Kanpur for microbeam experiments. We also acknowledge NIT Patna administration and the Department of Physics, for supporting and felicitating the experiments at IIT Kanpur and elsewhere.

References

- I.P. Jain, G. Agarwal, Ion beam induced surface and interface engineering, Surf. Sci. Rep. 66 (2011) 77–172, <https://doi.org/10.1016/j.surfrep.2010.11.001>.
- V. Heera, J. Stoemenos, F.L. Kogler, W. Skrupa, Amorphization and recrystallization of 6H-SiC by ion-beam irradiation, J. Appl. Phys. 77 (1995) 2999–3009, <https://doi.org/10.1063/1.358649>.
- T. Makarova, F. Palacio, Carbon-Based Magnetism, Elsevier, Amsterdam, 2006.
- R. Höhne, P. Esquinazi, Can Carbon Be Ferromagnetic, Adv. Mater. 14 (2002) 753–756, [https://doi.org/10.1002/1521-4095\(20020517](https://doi.org/10.1002/1521-4095(20020517)
- P. Esquinazi, A. Setzer, R. Höhne, C. Semmelhack, Y. Kopelevich, D. Spemann, T. Butz, B. Kohlstrunk, M. Lösche, Ferromagnetism in oriented graphite samples, Phys. Rev. B 66 (2002), 024429, <https://doi.org/10.1103/PhysRevB.66.024429>.
- J. Cervenka, M.I. Katsnelson, C.F.J. Flipse, Room-temperature ferromagnetism in graphite driven by two-dimensional networks of point defects, Nat. Phys. 5 (2009) 840–844, <https://doi.org/10.1038/nphys1399>.
- O.V. Yazayev, Emergence of magnetism in graphene materials and nanostructures, Rep. Prog. Phys. 73 (2010), 056501, <https://doi.org/10.1088/0034-4885/73/5/056501>.
- P.O. Allemand, K.C. Khemani, A. Koch, F. Wudl, K. Holczer, S. Donovan, G. Grüner, J.D. Thompson, Organic Molecular Soft Ferromagnetism in a Fullerene_{C₆₀}, Science 253 (1991) 301–303, <https://doi.org/10.1126/science.253.5017.301>.
- J.M.D. Coey, M. Venkatesan, C.B. Fitzgerald, A.P. Douvalis, I.S. Sanders, Ferromagnetism of a graphite nodule from the Canyon Diablo meteorite, Nature 420 (2002) 156–159, <https://doi.org/10.1038/nature01100>.
- P. Esquinazi, D. Spemann, R. Höhne, A. Setzer, K.-H. Han, T. Butz, Induced magnetic ordering by proton irradiation in graphite, Phys. Rev. Lett. 91 (2003), 227201, <https://doi.org/10.1103/PhysRevLett.91.227201>.
- P.O. Lehtinen, A.S. Foster, Y. Ma, A.V. Krashennnikov, R.M. Nieminen, Irradiation-induced magnetism in graphite: A density functional study, Phys. Rev. Lett. 93 (2004), 187202, <https://doi.org/10.1103/PhysRevLett.93.187202>.
- S. Talapatra, P.G. Ganesan, T. Kim, R. Vajtai, M. Huang, M. Shima, G. Ramanath, D. Srivastava, S.C. Deevi, P.M. Ajayan, Irradiation induced magnetism in carbon nanostructures, Phys. Rev. Lett. 95 (2005), 097201, <https://doi.org/10.1103/PhysRevLett.95.097201>.
- H. Xia, W. Li, Y. Song, X. Yang, X. Liu, M. Zhao, Y. Xia, C. Song, T.W. Wang, D. Zhu, J. Gong, Z. Zhu, Tunable Magnetism in Carbon-ion-implanted highly oriented pyrolytic graphite, Adv. Mater. 20 (2008) 4679–4683, <https://doi.org/10.1002/adma.200801205>.
- M.A. Ramos, J. Barzola-Quiquia, P. Esquinazi, A. Muñoz-Martin, A. Climent-Font, M. García-Hernández, Magnetic properties of graphite irradiated with MeV ions, Phys. Rev. B 81 (2010), 214404, <https://doi.org/10.1103/PhysRevB.81.214404>.
- N. Shukla, M. Sarkar, N. Banerji, A.K. Gupta, H.C. Verma, Inducing large ferromagnetic ordering in graphite by 1 MeV ¹²C⁺ ion irradiation, Carbon 50 (2012) 1817–1822, <https://doi.org/10.1016/j.carbon.2011.12.031>.
- K. Kusakabe, M. Maruyama, Magnetic Nanographite, Phys. Rev. B 67 (2003), 092406, <https://doi.org/10.1103/PhysRevB.67.092406>.
- X. Yang, G. Wu, Itinerant flat-band magnetism in hydrogenated carbon nanotubes, Nano Lett 3 (2009) 1646–1650, <https://doi.org/10.1021/nn900379y>.
- A.L. Friedman, H. Chun, Y.J. Jung, D. Heiman, E.R. Glaser, L. Menon, Possible room-temperature ferromagnetism in hydrogenated carbon nanotubes, Phys. Rev. B 81 (2010), 115461, <https://doi.org/10.1103/PhysRevB.81.115461>.
- J. Barzola-Quiquia, W. Böhlmann, P. Esquinazi, A. Schadewitz, A. Ballestar, S. Dusari, L. Schultze-Nobre, B. Kersting, Enhancement of the ferromagnetic order of graphite after sulphuric acid treatment, Appl. Phys. Lett. 98 (2011), 192511, <https://doi.org/10.1063/1.3590924>.
- T.L. Makarova, A.L. Shelankov, I.T. Serenkov, V.I. Sakharov, Magnetism in graphite induced by irradiation of hydrogen or helium ions – A comparative study, Phys. Status Solidi B 247 (2010) 2981–2988, <https://doi.org/10.1002/pssb.201000114>.
- T.L. Makarova, A.L. Shelankov, I.T. Serenkov, V.I. Sakharov, D.W. Boukhvalov, Anisotropic magnetism of graphite irradiated with medium energy hydrogen and helium ions, Phys. Rev. B 83 (2011), 085417, <https://doi.org/10.1103/PhysRevB.83.085417>.
- J. Barzola-Quiquia, R. Höhne, M. Rothermel, A. Setzer, P. Esquinazi, V.A. Heera, Comparison of the magnetic properties of proton- and iron-implanted graphite, Eur. Phys. J. B 61 (2008) 127–130, <https://doi.org/10.1140/epjb/e2008-00047-7>.
- H.W. Kroto, J.R. Heath, S.C.O. Brien, R.F. Curl, R.E. Smalley, C₆₀: Buckminsterfullerene, Nature 318 (1985) 162–163, <https://doi.org/10.1038/318162a0>.
- W. Krätschmer, L.D. Lamb, K. Fostiropoulos, D.R. Huffman, Solid C₆₀: A new form of Carbon, Nature 347 (1990) 354–358, <https://doi.org/10.1038/347354a0>.
- H.W. Kroto, A.W. Allaf, S.P. Balm, C₆₀: Buckminsterfullerene, Chem. Rev. 91 (1991) 1213–1235, <https://doi.org/10.1021/cr00006a005>.
- M. Prato, Fullerene chemistry for materials science applications, J. Mater. Chem. 7 (1997) 1097–1109, <https://doi.org/10.1039/A700080D>.
- L. Forró, L. Mihály, Electronic Properties of doped Fullerenes, Rep. Prog. Phys. 64 (2001) 649–699, <https://doi.org/10.1088/0034-4885/64/5/202>.
- Y. Murkami, H. Suematsu, Magnetism of C₆₀ induced by photo assisted oxidation, Pure & Appl. Chem. 68 (1996) 1463–1467, <https://doi.org/10.1351/pac199668071463>.
- R.A. Wood, M.H. Lewis, M.R. Lees, S.M. Bennington, M.G. Cain, N. Kitamura, Ferromagnetic Fullerene, J. Phys. Cond. Mat. 14 (2002) L385, <https://doi.org/10.1088/0953-8984/14/22/L01>.
- T.L. Makarova, K.H. Han, P. Esquinazi, R.R. Da Silva, Y. Kopelevich, I. B. Zakhrova, B. Sundqvist, Magnetism in photopolymerized fullerenes, Carbon 41 (2003) 1575–1584, [https://doi.org/10.1016/S0008-6223\(03\)00082-4](https://doi.org/10.1016/S0008-6223(03)00082-4).
- T.L. Makarova, O.E. Kvyatkovskii, I.B. Zakhrova, S.G. Buga, A.P. Volkov, A. L. Shelanko, Laser controlled magnetism in hydrogenated fullerene films, J. Appl. Phys. 109 (2011), 083941, <https://doi.org/10.1063/1.3581105>.
- K. Narumi, Y. Xu, K. Miyashita, H. Naramoto, Effect of ion irradiation in C₆₀ thin Films, Eur. Phys. J. D 24 (2003) 385–388, <https://doi.org/10.1140/epjd/e2003-00150-5>.
- N. Bajwa, K. Dharamvir, V.K. Jindal, A. Ingale, D.K. Avasthi, R. Kumar, A. Tripathi, Swift heavyion induced modification of C₆₀ thin films, J. Appl. Phys. 94 (2003) 326–333, <https://doi.org/10.1063/1.1581381>.

- [34] A. Kumar, D.K. Avasthi, J.C. Pivin, A. Tripathi, F. Singh, Ferromagnetism induced by Heavy ion irradiation in fullerene films, *Phys. Rev. B* 74 (2006), 153409, <https://doi.org/10.1103/PhysRevB.74.153409>.
- [35] S. Mathew, B. Satpati, B. Joseph, B.N. Dev, R. Nirmala, S.K. Malik, R. Kesavamoorthy, Magnetism in C_{60} Films induced by proton irradiation, *Phys. Rev. B* 75 (2007), 075426, <https://doi.org/10.1103/PhysRevB.75.075426>.
- [36] K.W. Lee, H. Kweon, C.E. Lee, Field Induced Transition from Room-Temperature Ferromagnetism to Diamagnetism in Proton Irradiated Fullerene, *Adv. Mater.* 25 (2013) 5663–5667, <https://doi.org/10.1002/adma.201301635>.
- [37] Y. Wang, P. Pochet, C.A. Jenkins, E. Arenholz, G. Bukalis, S. Gemming, M. Helm, S. Zhou, Defect Induced Magnetism in graphite through neutron irradiation, *Phys. Rev. B* 90 (2014), 214435, <https://doi.org/10.1103/PhysRevB.90.214435>.
- [38] Interactions of Ions with Matter, <http://www.srim.org>.
- [39] J.F. Ziegler, J.P. Biersack, U. Littmark, *The Stopping and Range of Ion in Solids*, Pergamon, New York, 1985.
- [40] J.F. Ziegler, J.P. Biersack, M.D. Ziegler, *The stopping and range of ion in matter, Ion Implantation Technology Press, London, 2008*.
- [41] R.R. Nair, I-L Tsai, M. Sepioni, O. Lehtinen, J. Keinonen, A.V. Krasheninnikov, A. H Castro Neto, M.I. Katsnelson, A.K. Geim, I.V. Grigorieva, Dual origin of defect Magnetism in graphene and its reversible switching by molecular doping, *Nature Commun* 4 (2013) 2010, <https://doi.org/10.1038/ncomms3010>.
- [42] S. Maurya, L.C. Tribedi, R. Maringanti, Engineering of Silicon/HfO₂ Interface by variable energy proton irradiation, *Appl. Phys. Lett.* 105 (2014), 071605, <https://doi.org/10.1063/1.4893731>.
- [43] Y. Wang, Y. Liu, G. Wang, W. Anwand, C.A. Jenkins, E. Arenholz, F. Munnik, O. D. Gordan, G. Salvan, D.R.T. Zahn, X. Chen, S. Gemming, M. Helm, S. Zhou, Carbon p Electron Ferromagnetism in Silicon Carbide, *Nat. Sci. Rep.* 5 (2015) 8999, <https://doi.org/10.1038/srep08999>.
- [44] A.I. Podlivaev, L.A. Openova, Thermal Annealing of Stone-Wales Defects in Fullerenes and Nanotubes, *Phys. Solid State* 60 (2018) 162–166, <https://doi.org/10.1134/S1063783418010183>.

PAPER

Stability analysis of two-fluid dark energy models

B Mishra^{5,1} , Fakhreeh Md Esmaeili², Pratik P Ray³ and S K Tripathy⁴

Published 4 February 2021 • © 2021 IOP Publishing Ltd

[Physica Scripta, Volume 96, Number 4](#)

Citation B Mishra *et al* 2021 *Phys. Scr.* **96** 045006

DOI 10.1088/1402-4896/abdf82

References ▾

Article metrics

123 Total downloads



Submit

[Submit to this Journal](#)

Permissions

[Get permission to re-use article](#)

Share this article



You may also like

JOURNAL ARTICLES

[Comprehensive Structural Analysis Identifies the Relationships Between the Electrical Characteristics of Environmentally Friendly NBTMn-BAl-NaNb Ceramics](#)

Physica Scripta


Article and author information

Abstract

In this paper, we have studied the stability of the cosmological models with dark energy and

Abstract

References



 Snipping Tool ... X
Screenshot copied to clipboard and saved
Select here to mark up and share.

[Submitted on 9 Apr 2021]

Wormhole solutions in $f(R)$ Gravity

B.Mishra, A.S. Agrawal, S.K. Tripathy, Saibal. Ray

In this work, we have studied the traversable wormholes geometry in $f(R)$ theory gravity, where R be the Ricci scalar. The wormhole solution for some assumed $f(R)$ functions have been presented. The assumption of $f(R)$ is based on the fact that its behaviour changed with an assumed parameter α rather than the deceleration parameter. Three models are presented based on the physically motivated shape function and their behaviours are studied.

Comments: 12 pages, 12 figures, Accepted Version IJMPD
Subjects: **General Relativity and Quantum Cosmology (gr-qc)**
Cite as: arXiv:2104.05440 [gr-qc]
(or arXiv:2104.05440v1 [gr-qc] for this version)
<https://doi.org/10.48550/arXiv.2104.05440> 
Journal reference: Int. J. Mod. Phys. D, 30, 2150061 (2021)
Related DOI: <https://doi.org/10.1142/S0218271821500619> 

Submission history

From: Bivudutta Mishra Dr. [\[view email\]](#)
[v1] Fri, 9 Apr 2021 04:34:51 UTC (213 KB)

Access Paper:

- [View PDF](#)
- [TeX Source](#)
- [Other Formats](#)

[View license](#)

Current browse context:

gr-qc

[< prev](#) | [next >](#)
[new](#) | [recent](#) | [2021-04](#)

References & Citations

- [INSPIRE HEP](#)
- [NASA ADS](#)
- [Google Scholar](#)
- [Semantic Scholar](#)

Export BibTeX Citation

Bookmark



Cookies Notification

We use cookies on this site to enhance your user experience. By continuing to browse the site, you consent to the use of our cookies. [Learn More](#)



I Agree

International Journal of Modern Physics D | Vol. 30, No. 16, 2140005 (2021)

No Access

Figures References Related Details

Cosmological models with a hybrid scale factor

S. K. Tripathy, B. Mishra , Maxim Khlopov, and Saibal Ray

<https://doi.org/10.1142/S0218271821400058> | Cited by: 13 (Source: Crossref)

< Previous

Next >

This article is part of the issue:

SPECIAL ISSUE: Challenging Problems of Particle Physics and Astrophysics

Editor: Maxim Yu. Khlopov

PDF/EPUB



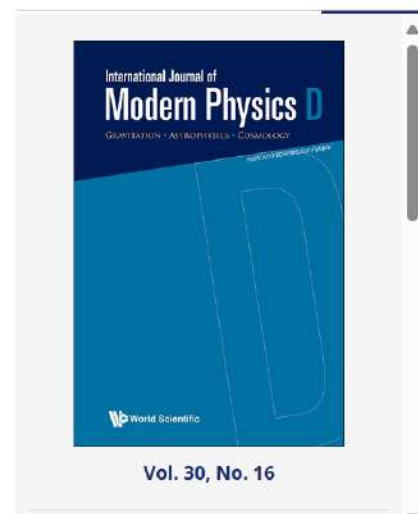
Tools

< Share

Quote Cite



Recommend To Library



Vol. 30, No. 16

Abstract

Access through Indira Gandhi Institute o...

Access through another institution

Article preview

Abstract

Introduction

Section snippets

References (52)

Cited by (112)



Physics of the Dark Universe

Volume 36, June 2022, 101020



Dynamical system analysis for accelerating models in non-metricity $f(Q)$ gravity

S.A. Narawade ^{a,1}, Laxmipriya Pati ^{a,1}, B. Mishra ^{a,1}, S.K. Tripathy ^{b,1}

Show more

Add to Mendeley Share Cite

<https://doi.org/10.1016/j.dark.2022.101020>

Get rights and content

Abstract

Recommended articles

Accelerating scenarios of mass universe in $f(R, L_m)$ -gravity

New Astronomy, Volume 100, 2023, Ar Dinesh Chandra Maurya

Generalized Chaplygin gas and accelerating universe in $f(Q)$

Physics of the Dark Universe, Volume 3 Gaurav N. Gadbail, ..., P.K. Sahoo

Testing $F(Q)$ gravity with red space distortions

Physics of the Dark Universe, Volume 3 Bruno J. Barros, ..., Nelson J. Nunes

Show 3 more articles

Article Metrics

FEEDBACK